

Influence of Masonry Panels on the Life-Cycle Expected Performance Functions of Multi-Story RC Frames

R. Pérez-Martínez

Autonomous University of Hidalgo, Mexico

L. Esteva

Institute of Engineering, National University of Mexico, Mexico



SUMMARY:

A study is presented about the influence of infill masonry panels on the life-cycle expected performance functions of multi-story reinforced concrete frames exposed to severe seismic hazard conditions. It is done, comparing the present values of expected damage functions of a sample including the same reinforced concrete rigid-frame system: in one case there is not any infill-wall; in the second case, there are masonry infill-walls at all stories, except the first one, at the two exterior frames in planes parallel to the direction of ground motion, while in the third case infill-walls are inserted at all stories of the exterior frames of the building. The hysteretic behavior and damage model used here for concrete elements and for masonry walls take into account the strength and stiffness degradation as functions of damage accumulation.

Keywords: Masonry walls, life-cycle optimization, seismic performance, seismic risk, structural reliability.

1. INTRODUCTION

The influence on the structural performance of infilled-frames subjected to lateral loads has been recognized at least since the late 1930s [Rathbun, 1938]; it has been the subject of many experimental studies around the world, considering different lateral and vertical load conditions and taking into account particular characteristics of masonry components, construction methods, block types that vary from one region to another (*e.g.* Polyakov, 1956; Holmes, 1961; Stafford-Smith, 1962; Liao, 1964; Esteva, 1966; among others), as summarized by Crisafulli (1997).

In addition, experimental studies done by Tomažević *et al.* (1996) on 32 half-scale masonry walls subjected to different lateral load patterns (statically and dynamically) at two levels of vertical loads, showed significant differences in lateral resistance and initial stiffness. As a general rule, they measured higher resistance and larger ultimate displacement for monotonically loading than for the other load patterns.

This study is oriented to presenting some information about the expected life-cycle benefits that can be obtained from the use of non reinforced and horizontally-reinforced confined masonry panels as structural infilling elements in rigid frame multistory buildings built at sites exposed to significant seismic hazard conditions. For this purpose, the nonlinear behavior of confined masonry panels subjected to cyclic loads is represented by the model proposed by Pérez-Martínez and Esteva (2011), based on experimental information provided by cyclic load tests performed at the National Center for Disaster Prevention of Mexico (CENAPRED) on full-scale confined masonry panels [Aguilar *et al.*, 1996; Alcocer and Zepeda, 1999], where reinforcement confinement details and joint mortar properties were defined in compliance with the requirements established by the 1993 issue of the Mexico City Building Code [MCBC, 1993].

2. SEISMIC RELIABILITY ANALYSIS

The life-cycle framework adopted here for the evaluation of expected performance functions is taken from Esteva *et al.* (2002). Let Q designate an intensity measure of a seismic ground motion acting on a structural system and Z a quantitative indicator of the performance of that system when subjected to that action. For many applications, Z is a safety factor equal to $\ln(C/D)$, where C is the (drift) capacity of the system and D is the corresponding seismic drift demand. For a given combination of structural system and seismic excitation, C and D are determined by means of a pushover analysis and a step-by-step analysis, respectively.

Following Cornell (1969), the seismic reliability level of a system is expressed in terms of the safety index β , equal to \bar{Z}/σ_Z where \bar{Z} is the expected value of Z (defined in the foregoing paragraph) and σ_Z is its standard deviation. In addition, the probability of failure p_F is assumed to be approximately equal to $\Phi(-\beta)$, where $\Phi(\cdot)$ is the normal standard cumulative probability distribution function.

2.1. Constitutive functions

Constitutive functions for reinforced concrete members are taken from Campos and Esteva (1997) and the hysteretic behavior and damage model for masonry walls from Pérez-Martínez and Esteva (2011), presented in Fig. 2.1. Both models are based on the concept of damage accumulation proposed by Wang and Shah (1987); they take into account the strength and stiffness degradation and are incorporated in program Drain 2D [Powell, 1973].

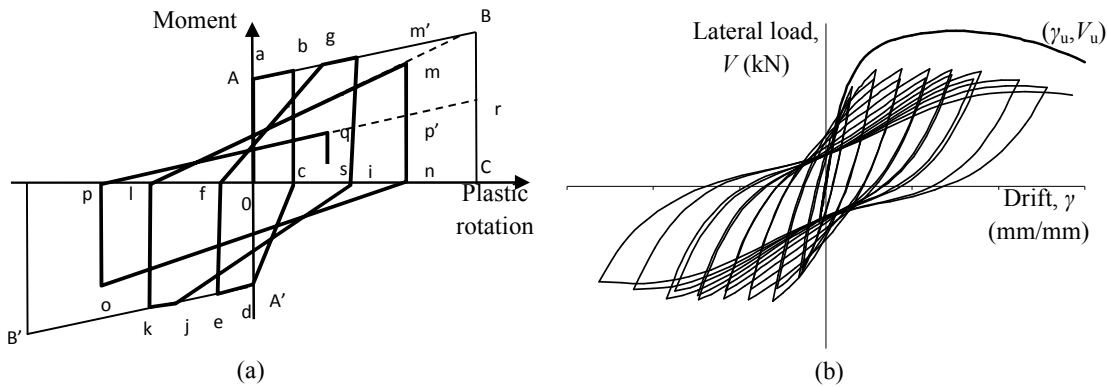


Figure 2.1 Hysteretic models of a) RC element ends and b) Confined masonry wall

2.2. Capacity of the system and seismic demand

In order to estimate the lateral deformation capacity of each system, a pushover analysis with constant displacement configuration was performed on the corresponding detailed model. The displacement configuration used for this purpose was taken equal to that determined from conventional (square root of sum of squares) superposition of linear modal responses for the specified seismic-design spectrum; the shape of the resulting configuration of lateral displacements was kept constant while the frame was forced into the inelastic range. For this analysis, the excitation was a base acceleration growing slowly as a linear function of time; all gravitational loads and mechanical properties were taken equal to their expected values. The lateral deformation capacity was taken as equal to that corresponding to a reduction of 20% in the maximum base shear force reached by the RC frame during the pushover analysis.

Two measures of the seismic demand were considered:

- a) The global lateral distortion, equal to the ratio of the peak absolute value of the amplitude of the roof displacement relative to that of the base of the structure, or

- b) The local lateral distortion, equal to the ratio of the peak absolute value of the amplitude of the first story displacement relative to that of the base of the structure.

Case (b) will be used when the soft-story mechanism is produced. Both cases are obtained by dynamic nonlinear analyses of MDOF systems subjected to the ground motion accelerations time histories considered. For each system studied, a sample of dynamic response time histories was obtained, where both the system properties and the ground motion time histories were taken as random: the former were generated by means of Monte Carlo simulation, and the latter are either actual records or scaled versions of them.

2.3. Normalized intensity measure

A normalized intensity measure is defined as $Q = m \cdot S_a / V_y$, where S_a is the linear pseudo-acceleration response ordinate for the fundamental period of the system of interest, m is the mass of that system, and V_y is the yield value of the base shear force obtained by least squares fitting to the base-shear vs. lateral displacement function resulting from a pushover analysis.

2.4. Seismic hazard function

The seismic hazard function $v_Y(y)$ is defined here as the annual rate of occurrence of earthquakes with intensities Y greater than any given value, y , at the site; it can be represented as follows:

$$v_Y(y) = K \cdot y^{-r} \left[1 - \left(\frac{y}{y_1} \right)^\varepsilon \right] \text{ if } y < y_1 ; v_Y(y) = 0, \text{ otherwise.} \quad (2.1)$$

Here, y is a value of the earthquake intensity, measured by the ordinate of the linear pseudo-acceleration response spectrum for the fundamental period of the system of interest; r , y_1 , and ε are parameters determined by site-specific seismic hazard studies.

2.5. Seismic vulnerability functions

According to Esteva *et al.*, (2002), the vulnerability function $\delta(y)$ can be expressed as the sum of the contributions of the expected damage costs in the cases of failure and survival of the system:

$$\delta(y) = \delta_F \cdot p_F(y) + \bar{\delta}(y|S) \cdot [1 - p_F(y)] \quad (2.2)$$

where

$$\bar{\delta}(y|S) = (\lambda + r_1) \sum_i r_{ci} \cdot \bar{g}(\Psi_i) \quad (2.3)$$

In these equations, $p_F(y)$ is the failure probability under the action of an earthquake with intensity y , δ_F is the expected cost of failure in case it occurs, and $\bar{\delta}(y|S)$ is the expected cost of damage, conditional to survival. Both δ_F and $\bar{\delta}(y|S)$ are normalized with respect to the initial construction cost, C_0 .

In order to obtain the expected damage cost conditional to survival, $\bar{\delta}(y|S)$, it is necessary to segregate the initial total cost C_0 into the contributions of the different system segments, such as: structural frame, partitions and similar elements, installations, and floor systems and it is done according to Sierra (2002), Ismael (2003), Pérez-Martínez and Esteva (2012).

3. LIFE-CYCLE OBJECTIVE FUNCTION

For purposes of life-cycle utility-based decision making, an objective function must be defined. Following Esteva (1969) and Rosenblueth (1976), the utility function for a system which is repaired or rebuilt immediately after each damaging earthquake, using the same specifications as the original

system, can be expressed by Eq. 3.1, where α is a vector formed by the values of the parameters that determine the relevant mechanical properties of the system to be designed:

$$U = C_0(\alpha) + \frac{D_0(\alpha)}{\gamma} \quad (3.1)$$

Here, $C_0(\alpha)$ is the initial cost function, D_0 is the expected cost of damage and failure per unit time (year), and γ is an adequate discount (interest) rate. D_0 depends on both the seismic activity at the site of interest and the damage function $\delta(y)$, which expresses the expected cost of damage as a fraction of C_0 for an earthquake with intensity equal to y . $D_0(\alpha)/\gamma$ is the present value of the expected cost of damage, which is estimated as the sum of the contributions of the conditions of survival and failure, identified in Eqs. 3.2 – 3.4 by subscripts S and F , respectively:

$$D_0(\alpha) = [\Delta_S + \Delta_F] \cdot C_0(\alpha) \quad (3.2)$$

where

$$\Delta_S = \int \left| \frac{d\nu_y(y)}{dy} \right| \cdot \bar{\delta}(y|S) \cdot [1 - p_F(y)] dy \quad (3.3)$$

$$\Delta_F = \int \left| \frac{d\nu_y(y)}{dy} \right| \cdot \delta_F \cdot p_F(y) dy \quad (3.4)$$

4. ILLUSTRATIVE EXAMPLE

The illustrative example compares the present values of expected damage functions of a sample including the same reinforced concrete rigid-frame system: in one case there is not any infill-wall; in the second case, there are masonry infill-walls at all stories, except the first one, at the two exterior frames in planes parallel to the direction of ground motion, while in the third case infill-walls are inserted at all stories of the exterior frames of the building. The resulting configurations are shown in Fig. 4.1. The structural systems are located at a firm ground and were designed in accordance with the applicable seismic design regulations established for seismic Zone D by the Civil Works Design Handbook (Manual de Diseño de Obras Civiles, MDOC, 1993).

The building is regular both in plan and in elevation (Fig. 4.1) located at a firm ground site, base-shear coefficient of 0.1, and a seismic force reduction factor of 4.0. They are defined in terms of nominal values of both the gravitational loads and the mechanical properties of the structural members. The geometrical properties of the structural members are summarized in Table 4.1.

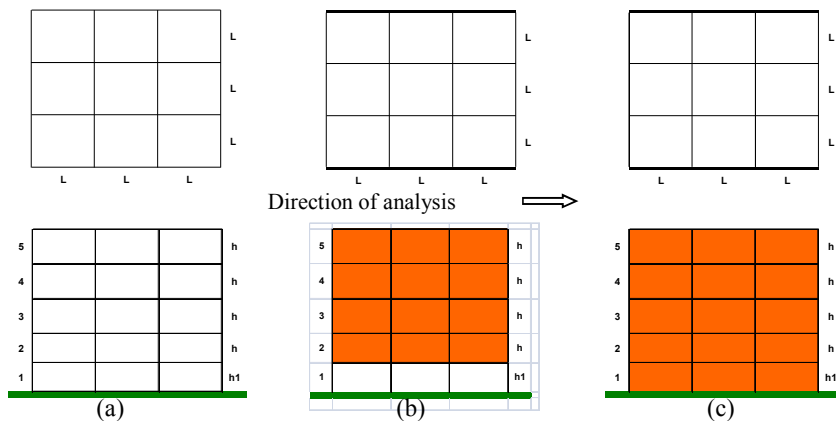


Figure 4.1. General dimensions of cases studied; $L=6.0$ m, $h=3.0$ m, $h_1=4.0$ m.

Table 4.1. Geometry of columns and beams of cases studied: $d = \text{depth}$, $b = \text{width}$.

Element	Story	Cross section $d \times b$ (mm)
Columns	1-2	500 x 500
	3-5	450 x 450
Beams	1-2	250 x 500
	3-5	200 x 500

In order to evaluate influence of masonry panels on the life-cycle expected performance functions of multi-story RC frames, three cases were selected: (1) bare frame system; (2) soft-story system; and (3) RC frame with masonry-infill in all panels. Additionally, two options of masonry panels are considered: (a) without horizontal reinforcement (M2); and (b) with reinforcement bars at the horizontal joints, a reinforcement ratio of 0.182% of the vertical cross section of the panel (M4) (See Table 4.2). The infill panels are built with traditional hand-made solid clay bricks [Aguilar *et al.*, 1996], which are modeled taking into account the strength and stiffness degradation as functions of damage accumulation (Sec. 2.1).

Table 4.2 Cases studied: bare frame, soft-story and RC frame with masonry-infill in all panels

Case	Horizontal reinforcement ratio of the masonry wall	ID	T_0 (s) using expected values
Bare frame	--	BF	0.88
Soft-story	--	SS-M2	0.55
	Maximum	SS-M4	
Masonry-infill in all panels	--	FI-M2	0.28
	Maximum	FI-M4	

4.1. Selection of seismic excitations

Fig. 4.2 shows three typical ground motion acceleration time histories recorded at hard-rock sites in the Pacific coast of Mexico (Acapulco area) and the response spectra for a larger sample, for 5 percent damping ratio [Pérez-Martínez and Esteva, 2012].

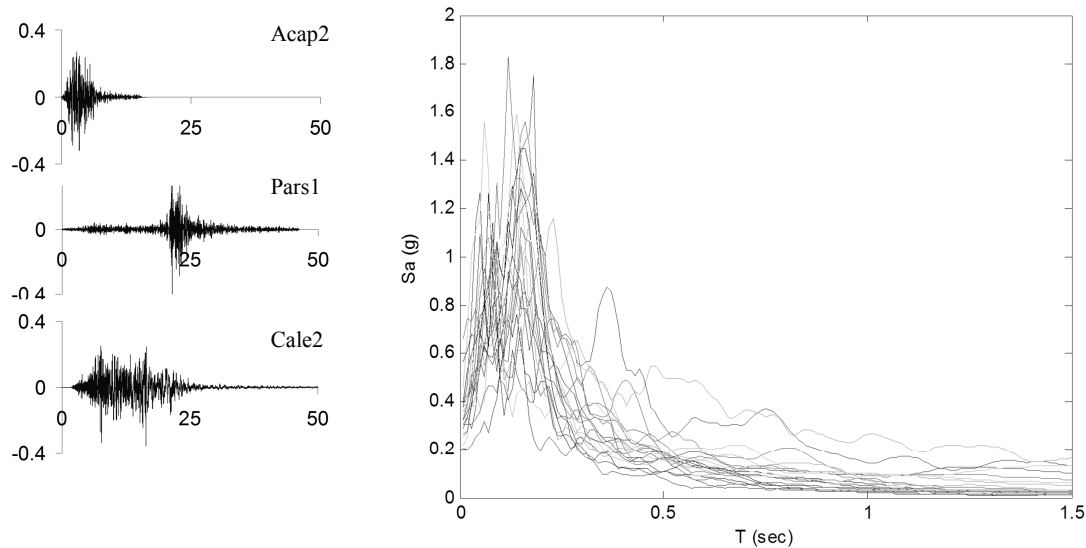


Figure 4.2 Typical ground motion acceleration time histories recorded at hard-rock sites in the Pacific coast of Mexico (Acapulco area) and their response spectra for 5 percent damping ratio. T is the natural period of vibration of the system considered.

4.2. Seismic reliability analysis

Lateral deformation capacity is obtained from a pushover analysis (C, Sec. 2) and it is presented in Fig. 4.3 where it can be observed, among other things, that the horizontal reinforcement in the masonry panel produces an increase of about 60 percent in the base-shear strength of the building; however, a drastic decrease in the base-shear is observed for a deformation much smaller than the deformation capacity of all the other specimens.

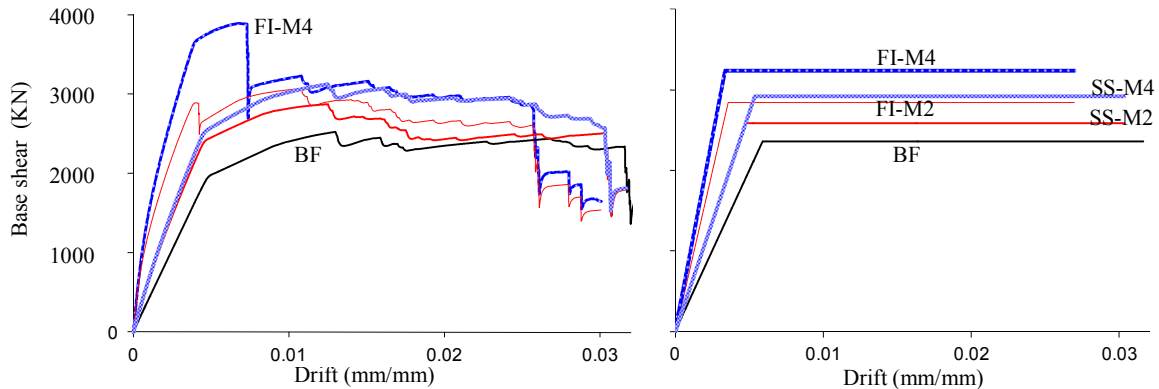


Figure 4.3 Pushover analysis and its corresponding elasto-plastic fitting for cases studied (C, Sec. 2).

Peak values of the global distortions (seismic demand D , Sec. 2) of the different systems are presented in Fig. 4.6. As expected, the largest global seismic demands are experienced by system BF, which has a deformation capacity not much larger than the other systems.

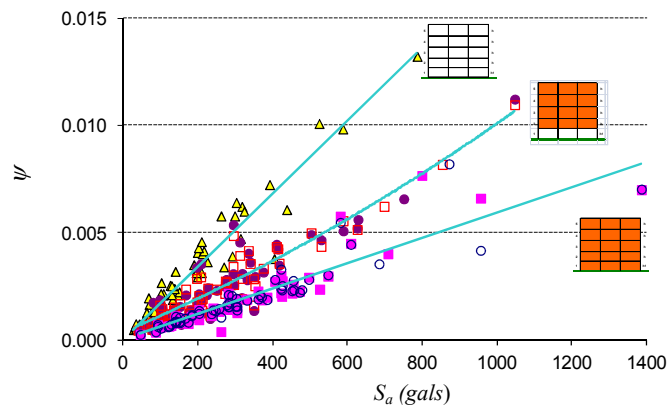


Figure 4.4 Peak values of global distortions ψ of detailed models of the systems (D, Sec. 2) vs. linear pseudo-acceleration response ordinates for the fundamental period of the system of interest, S_a .

The reliability functions $\beta(Q)$ for the systems considered were determined for all the systems, according to the definition presented in Section 2; the results are shown in Figure 4.5.

4.3. Life-cycle analysis

The seismic hazard function is defined here as the annual rate of occurrence of intensities Y greater than any given value, y , at the site. Intensities are measured by the ordinate of the linear pseudo-acceleration response spectrum, for 5 percent damping, for the natural period, T , of the system considered. Figure 4.6 shows the seismic hazard functions for the three basic cases presented in Table 4.2; they were determined using computer program PSM [Ordaz *et al.*, 1996].

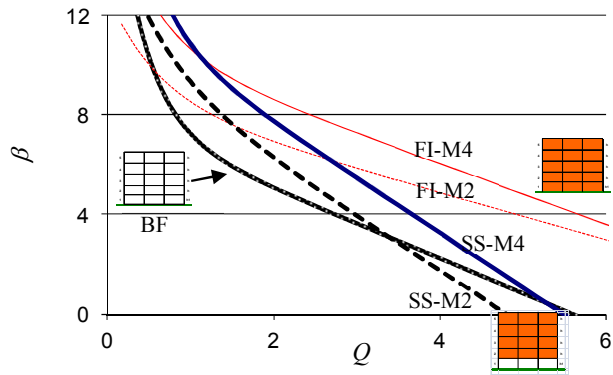


Figure 4.5 Reliability index β for cases studied as function of the normalized intensity measure Q .

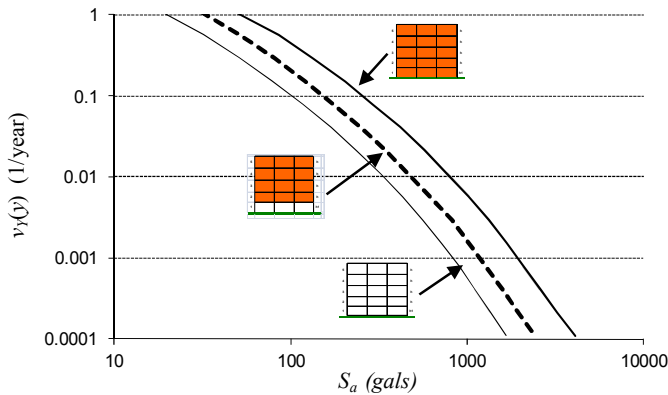


Figure 4.6 Annual rates of occurrence of earthquakes with intensities greater than γ at the site. T is determined using expected values of the mechanical properties of the system.

Figure 4.7 shows the expected damage functions conditional to survival for RC frame, partition wall and masonry wall (types M2 and M4, Table 4.2), determined in accordance with Eqns. 3.2 – 3.4. In this study, it is considered that the bare frame system BF is infilled with partition walls at all stories at the two exterior frames in planes parallel to the direction of ground motion. Partitions walls do not contribute to the strength and stiffness of the structural systems, but they contribute to the expected damage costs.

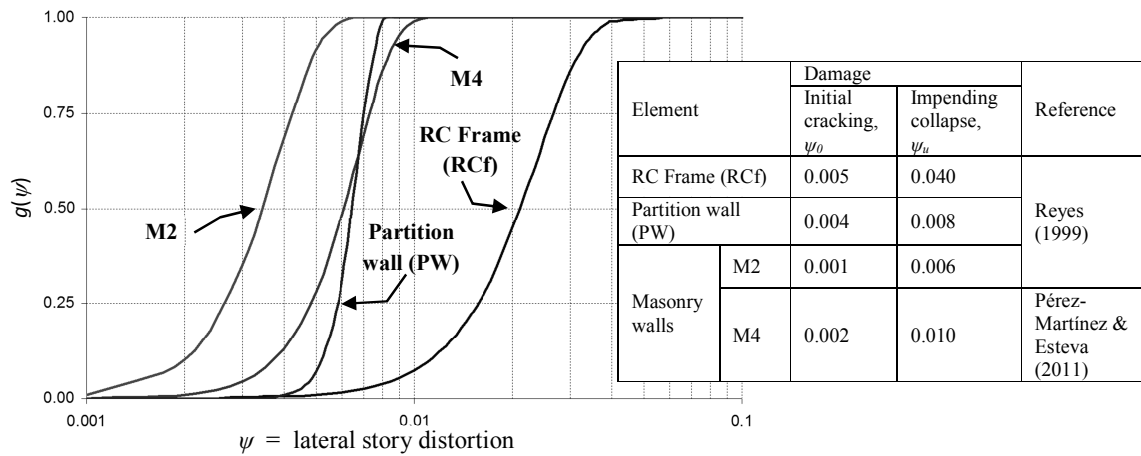


Figure 4.7 Expected damage functions of the systems studied, conditional to survival

In Table 4.3, the additional investment needed to replace the partition walls of the BF system by masonry walls (M2 or M4, Table 4.2) is presented for the three cases studied (Fig. 4.1)

Table 4.3. Initial costs of non-structural elements employed, and additional investments needed to replace masonry walls by partition walls (as percentage of C_0).

System	Masonry walls (A)	Partition wall (B)	Cost (C) = (A)+ (B)	Additional investment $\Delta i = C_i - C_1$
BF	0	2.40	2.40	0.00
SS-M2	3.60	0.48	4.08	1.68
SS-M4	3.78		3.78	1.38
FI-M2	4.50	0.00	4.50	2.10
FI-M4	4.73		4.73	2.33

Figure 4.8 shows present values of expected damage costs, determined in accordance with Section 3: (a) conditional to survival, $\Delta_S C_0 / \gamma$ and (b) failure, $\Delta_F C_0 / \gamma$. Finally, Figure 4.9 shows the life-cycle present values of structural systems: (a) without the *additional investment* Δi (Table 4.3) and (b) including Δi .

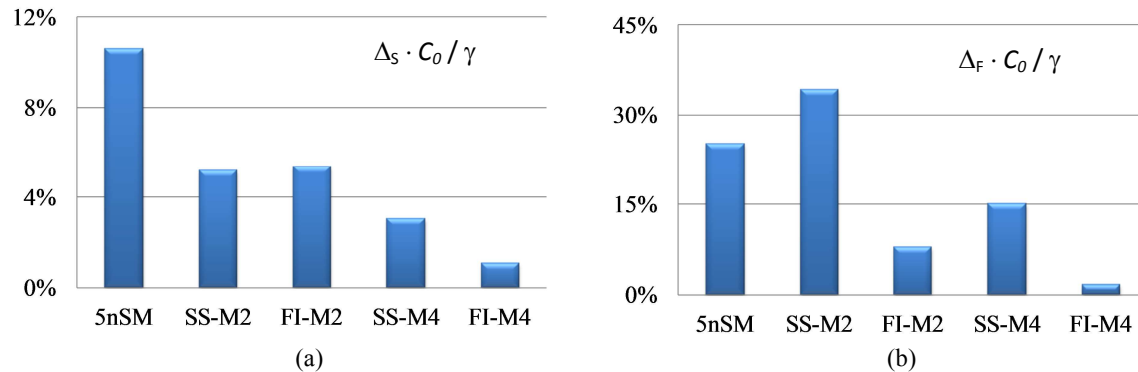


Figure 4.8 Present value of expected damage costs: (a) conditional to survival, $\Delta_S C_0 / \gamma$ and (b) failure, $\Delta_F C_0 / \gamma$.

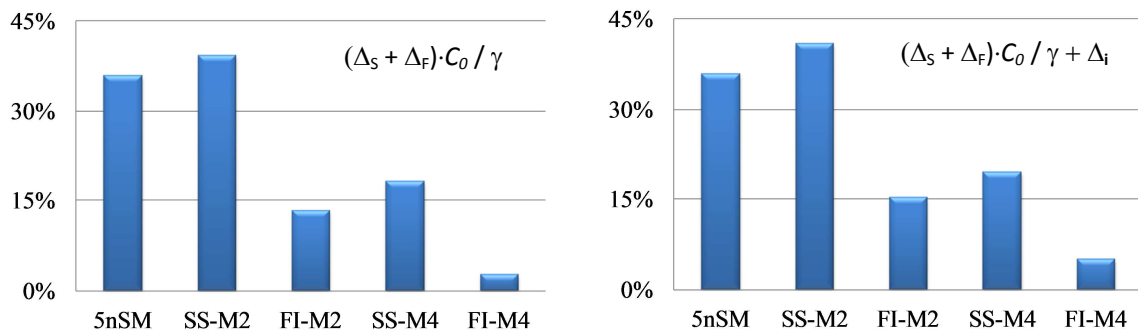


Figure 4.9. Life-cycle present values of structural systems: (a) without the *additional investment* Δi (Table 4.3) and (b) including Δi .

5. CONCLUDING REMARKS

A study is presented about the influence of infill masonry panels on the life-cycle expected performance functions of multi-story reinforced concrete frames exposed to severe seismic hazard conditions. For the cases studied, this influence is summarized in Fig. 4.9b. Similar studies are recommended considering different types of masonry elements, for systems located at sites with different seismic hazard conditions and types of soil.

Quantitative results have been presented about the influence of infill masonry panels on the following concepts:

- a) Lateral deformation capacity (Pushover analysis, Sec. 4.2, Fig. 4.3)
- b) Peak values of global distortions ψ of detailed models of the systems (Sec. 4.2, Fig. 4.4)
- c) Reliability index β as function of the normalized intensity measure Q (Sec. 4.2, Fig. 4.5)
- d) The natural period of vibration of the system considered and consequently the annual rates of occurrence of earthquakes with intensities greater than y at the site (Sec. 4.3, Fig. 4.6).

Additional results and details about the methodology and the coefficients used in this study are presented by Pérez-Martínez (2010).

ACKNOWLEDGEMENT

The first author would like to express his gratitude to the Mexican Ministry of Education for the financial support to present this paper.

REFERENCES

- Aguilar, G., Meli, R., Díaz, R., and Vazquez-del-Mercado, R. (1996). Influence of Horizontal Reinforcement on the Behavior of Confined Masonry Walls, *Proc. of the 11th World Conference on Earthquake Engineering*, Paper No. 1380, Acapulco, Mexico.
- Alcocer, S. M. and Zepeda, J. A. (1999). Behavior of Multi-Perforated Clay Bricks Walls under Earthquake-Type Loading, *Proc. of the 8th North American Masonry Conference*, Austin, TX, 235–246.
- Aslani, H. (2005). Probabilistic Earthquake Loss Estimation and Loss Disaggregation in Buildings, Ph.D. Thesis, Dept. of Civil and Environmental Engineering, Stanford University, Stanford, California.
- Campos, D. and Esteva, L. (1997). Modelo de Comportamiento Histéretico y de Daño para Vigas de Concreto Reforzado (Hysteretic Behavior and Damage Model for Reinforced Concrete Beams), *Proc. of XI National Conference on Earthquake Engineering*, Veracruz, Mexico (in Spanish).
- Cornell, A. C. (1969). A Probability-Based Structural Code, *Journal of the American Concrete Institute* **66**:12, 974–985.
- Crisafulli, F. J. (1997). Seismic Behaviour of Reinforced Concrete Structures with Masonry Infills, Ph.D. Thesis, Dept. of Civil Engineering, University of Canterbury, New Zealand.
- Esteva, L. (1966). Behavior Under Alternating Loads of Masonry Diaphragms Framed by Reinforced Concrete Members, *RILEM Symposium on the Effects of Repeated Loading on Materials and Structural Elements*, Mexico City.
- Esteva, L. (1969). Seismic Risk and Seismic Design Decisions, MIT Seminar on Seismic Design for Nuclear Power Plants, Cambridge, Massachusetts.
- Esteva, L., Díaz-López, O., García-Pérez, J., Sierra, G. and Ismael, E. (2002). Life-Cycle Optimization in the Establishment of Performance Parameters for Seismic Design. *Structural Safety*, **24**, 187-204.
- Holmes, M. (1961). Steel Frames with Brickwork and Concrete Infilling, *Proc. Institution of Civil Engineers* **19**, 473–478.
- Ismael, E. (2003). Funciones de Vulnerabilidad Sísmica para el Diseño Óptimo de Sistemas Marco-Muro (Seismic Vulnerability Function for Optimum Design of Wall-Frame Systems), Master Thesis, Graduate Program in Engineering, UNAM, México DF (in Spanish).
- Liao, H. M. (1964). Studies on Reinforced Concrete Shear Walls and Framed Masonry Shear Walls, Report, Engineering Research Institute, University of Tokyo, 89 pp.
- MCBC (1993). Reglamento de Construcciones del Distrito Federal (Mexico City Building Code), Gaceta Oficial del Departamento del Distrito Federal, Mexico DF (in Spanish)
- MDOC (1993). Manual de Diseño de Obras Civiles (Civil Works Design Handbook), Comisión Federal de Electricidad, Mexico (in Spanish).
- Ordaz, M. G., Aguilar, A., and Arboleda, J. (1996). PSM: Program for Computing Seismic Hazard, User's manual of computer program, Instituto de Ingeniería, UNAM, Mexico.
- Pérez-Martínez, R. (2010). Confiabilidad y Optimización para Diseño Sísmico de Edificios Considerando la Contribución de Muros de Mampostería (Reliability and Optimization for Seismic Design of Masonry-Infilled RC Frames). Ph.D Thesis, *Graduate Program in Engineering, UNAM, México DF* (in Spanish).
- Pérez-Martínez R. and Esteva L. (2011). A New Model for Hysteretic Behavior and Damage for Confined Masonry Walls. *Journal of Earthquake Engineering*. **15**:6, 942-958.

- Pérez-Martínez R. and Esteva L. (2012). Expected Performance Functions for Life-Cycle Analysis of Masonry-Infilled Reinforced Concrete Frames. *Journal of Earthquake Engineering*. **16:2**, 231-251.
- Polyakov S. V. (1956). Masonry on Framed Building; An Investigation into the Strength and Stiffness of Masonry Infillings, pub. by Gosudarstvennoe Izdatelstvo po Stroitelstvu I Arkhitekture, Moscow, (Translation into English by G. L. Cairns).
- Powell, G. H. (1973). Drain-2D User's Guide, Earthquake Engineering Research Center, University of California, Berkeley, California.
- Rathbun, J. C. (1938). Wind Forces on a Tall Building, *Proc. of the American Society of Civil Engineers*, **64**, 1335–1375.
- Reyes, J. C. (1999). El Estado Limite de Servicio en el Diseño Sísmico de Edificios (The Serviceability Limit State in the Seismic Design of Buildings), Ph.D. Thesis, Graduate Program in Engineering, UNAM, México DF (in Spanish).
- Rosenblueth, E. (1976). Optimum Design for Infrequent Disturbances, *ASCE Journal of Structural Division* **102:ST9**, 1807–1825.
- Sierra, G. (2002). Optimización en el Ciclo de Vida para Establecer Parámetros de Diseño Sísmico Basado en Desempeño (Life-Cycle Optimization for the Establishment of Performance-Based Seismic Design Parameters), Master Thesis, Graduate Program in Engineering, UNAM, Mexico City, Mexico (in Spanish).
- Stafford-Smith, B. (1962). Lateral Stiffness of Infilled Frames, *ASCE Journal of Structural Division* **88:ST6**, 183–199.
- Tomažević, M., Lutman, M., and Petković, L. (1996). Seismic Behavior of Masonry Walls: Experimental Simulation, *Journal of Structural Engineering* **122:9**, 1040–1047.
- Wang, M-L and Shah, S. P. (1987). Reinforced Concrete Hysteresis Model Based on Damage Concept, *Earthquake Engineering and Structural Dynamics* **15**, 993–1003.